INL/CON-23-73169-Revision-0

Techno-Economic Analysis of a Nuclear Reactor System coupled with a Liquid Metal Battery

November 2023

Samuel Jacob Root, Amey Shigrekar, Tyler L Westover

INL/CON-23-73169-Revision-0

Techno-Economic Analysis of a Nuclear Reactor System coupled with a Liquid Metal Battery

Samuel Jacob Root, Amey Shigrekar, Tyler L Westover

November 2023

Idaho National Laboratory
Idaho Falls, Idaho 83415

http://www.inl.gov

Prepared for the
U.S. Department of Energy
Under DOE Idaho Operations Office
Contract DE-AC07-05ID14517

Techno-Economic Analysis of a Nuclear Reactor System coupled with a Liquid Metal Battery

Sam J. Root, Amey Shigrekar, and Tyler L. Westover

*Hydrogen and Thermal Systems, Idaho National Laboratory, Idaho Falls, Idaho 83415,
Samuel.Root@inl.gov, Amey.Shigrekar@inl.gov, Tyler.Westover@inl.gov

INTRODUCTION

Decarbonization of the electrical grid is crucial to a sustainable future, but upsets the present paradigm for electricity generation. This poses a challenge to the nuclear power industry, which has historically supplied nearly exclusively baseload power. As renewable sources, which are intermittent, have relatively low capacity factors, and follow natural patterns rather than responding to consumption, expand to make up a larger share of domestic energy production, there is an increasing demand for Nuclear Reactor Systems (NRSs) to be more dynamic. Research to this end is multi-faceted; microreactors are smaller than the existing Nuclear Power Plants (NPP) fleet and have potential to change their power output more rapidly. Alternatively, a nuclear reactor may be paired with an Energy Storage System (ESS) to decouple electrical demand and generation altogether.

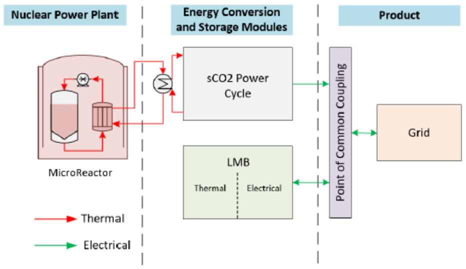

Fig. 1. Schematic drawing of the proposed ESS [1].

This study is a Techno-Economic Analysis (TEA) of a 20 $\mathrm{MW_{th}}$ High-Temperature Gas Reactor (HTGR) that is coupled to a 20 $\mathrm{MWh_e}$ Liquid Metal Battery (LMB) and the grid via a Supercritical Carbon-Dioxide (sCO_2) power cycle (Fig. 1). A pebble-bed HTGR is attractive for this system due to inherent safety and high operating temperature. The sCO_2 power cycle is able to very efficiently convert the thermal power from the reactor into electricity, and the LMB supports rapid charging and discharging, allowing the entire system to act as a black-start generator or peaking power station. In previous work, steady state and dynamic models for these systems were developed [1, 2]. These models can leveraged to complete a TEA of the ESS.

TECHNO-ECONOMIC ANALYSIS

TEA is an important bridge between research & development and deployment of a technology. It not only informs us whether a project in viable given current/projected markets, but, by including a sensitivity analysis can also tell us what future conditions foster success. Two key metrics are selected for the study: Levelized Cost of Electricity (LCOE) and Levelized Cost of Storage (LCOS).

LCOE, calculated by Eq. (1), is the average electricity sale price (in \$/kW-hr) at which the gross profit from the sCO_2 cycle covers the Capital Expenditure (CAPEX, \$), fixed operation and maintenance expenses ($\mathrm{O\&M_{fixed}}$,\$) and the generation costs. Generation costs are variable, and are calculated by the product of the Generation Price (GP, \$/kWh) and the electricity generated (E, kWh). The GP is, in this case, equal to the Levelized Cost of Heat (LCOH, \$/kWh) from the NRS divided by the thermal efficiency (η_{th}) of the sCO_2 cycle. Eq. (1) makes use of the Net Present Value (NPV) formula, expressed in Eq. (A.1) of the appendix, to discount future expenses and generation.

$$\mathrm{LCOE} = \frac{NPV\,(\mathrm{CAPEX} + \mathrm{O\&M_{fixed}} + \mathrm{GP} \times \mathrm{E})}{NPV(E)} \tag{1}$$

It is convenient to consider the NRS and sCO_2 cycle as separate entities. The NRS breaks even by always selling heat to the sCO_2 at the LCOH. The sCO_2 cycle profits by on average selling electricity to the grid above the LCOE. The sale price naturally fluctuates over the course of days and weeks and is correlated to demand.

A utility may look to increase the average sale price with the installation of an ESS such as an LMB. If the grid price falls below a certain threshold, *e.g.* the 'at cost' price, the electricity will instead be sold to the LMB at the Threshold Price (TP, \$/kWh). The LMB then stores the electricity and sells it when the grid price is higher. If it is able to, on average, sell the stored electricity to the grid at the LCOS, the ESS breaks even and the overall system yields a net gain.

$$\mathrm{LCOS} = \frac{NPV\,(\mathrm{CAPEX} + \mathrm{O\&M_{fixed}} + \mathrm{ECP} \times \mathrm{S})}{NPV(S)} \tag{2}$$

Eq. (2) is similar to Eq. (1) and represents the costs that need to be covered by the ESS. Charging costs are variable, and are defined by the amount of electricity stored and discharged (S, kWh) and the Electricity Charging Price (ECP, kWh), which is composed of the TP divided by the Round Trip Efficiency (RTE).

The methodology for determining inputs for the financial analysis is outlined in the following subsections. Most notably, the Installed Equipment Cost (IEC) for the systems is calculated and included in Table I. The IEC is the key contributor to the CAPEX, with future expenses discounted to represent the overnight cost equivalent.

Nuclear Reactor System

Numerous studies have been completed in recent years on the economics of nuclear power. The present work relies on a 2022 study that reported a LCOH in the range of 43.7$/MWth$ for microreactors (depending on the capacity factor) with an overnight capital cost of \$10.9k/kWe [5].

TABLE I. Installed Equipment Cost

System	Equipment	Unit Price ($)	IEC ($MM)	Obtained
LMB		-	6.49	-
	Mg Anode	50.1 k	-	-
	NaCl:KCl:MgCl$_2$ Electrolyte	12.5 k	-	-
	Sb Cathode	274.7 k	-	-
	Al$_2$O$_3$ Insulation	2.6 k	-	-
	SS304 Structure	53.4 k	-	-
sCO$_2$ Cycle		-	29.1	
	Turbine	4.73 MM	-	Eq. (3) [3]
	Main Compressor	1.45 MM	-	Eq. (4) [3]
	Re-compressor	1.69 MM	-	Eq. (4) [3]
	Primary Heat Exchanger	1.14 MM	-	Apsen EDR [4]
	High Temperature Recuperator	11.1 MM	-	Apsen EDR [4]
	Low Temperature Recuperator	1.74 MM	-	Apsen EDR [4]
	Air-Cooled Heat Sink	0.41 MM	-	Apsen EDR [4]
NRS	*HTGR Microreactor*	-	73.04	[5, Table 3]

Supercritical Carbon-Dioxide Power Cycle

The cycle studied in this work operates from 8.412 to 20.13 MPa and 36 to 750 °C. It is capable of converting 20 MW$_{th}$ from the NRS to 13.46 MW$_s$ at 49.2% thermal efficiency with 3.6 MW$_s$ being used for compression.

The cycle was modeled in Aspen HYSYS (Fig. 2), so price estimates for the heat exchangers could readily be obtained using Aspen Exchanger Design & Rating (EDR). The turbo-mechanical equipment is operated outside of the thermodynamic conditions available in Aspen Process Economic Analyzer (APEA), so literature was consulted to estimate the installed equipment cost for the compressors and turbine [3].

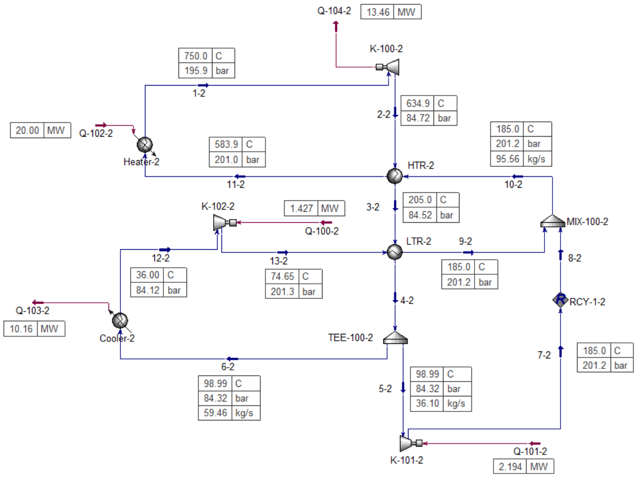

Fig. 2. HYSYS model of the sCO$_2$ power cycle [2].

Heat Exchangers

The sCO$_2$ cycle contains 4 heat exchangers: 1) A primary heat exchanger that extracts heat from the NRS primary coolant; 2) A high temperature recuperator that recovers heat from the turbine exhaust; 3) A low temperature recuperator that reheats the stream that was sent to the heat sink; and 4) An air cooled heat sink that cools a fraction of the exhaust stream;

Aspen EDR was used to determine a unit price for each exchanger. A variety of materials were investigated, including stainless steels and nickel alloys. EDR determined that carbon steel has sufficient mechanical properties for the two low temperature applications, however, literature consultation [6] presents chemical compatability concerns between sCO$_2$ and carbon steel due to carburization. As such, it was decided to select the next most economical material. 316 stainless steel was selected for the air cooled heat sink, while the three shell and tube heat exchangers used 22Cr5Ni3Mo steel.

Turbo-Machinery

The sCO$_2$ cycle has 3 turbo-mechanical components: 1) A turbine; 2) A main compressor that pressurizes the heat sink outlet stream; and 3) A re-compressor that pressurizes a fraction of the exhaust that bypasses the heat sink;

A literature source was identified that contains cost correlations for sCO$_2$ equipment [3]. Eq. (3) is a shaft power ($\dot{W}_{sh}$) to cost (C_t) correlation for sCO$_2$ turbine that is valid for turbines from 8 to 35 MW, and includes a high temperature (T_{max}) correction factor for turbines above 550°C.

$$C_t = \dot{W}_{sh}^{0.8}\left[406,200 + 4.618(T_{max} - 550)^2\right] \tag{3}$$

Eq. (4) is a similar correlation that provides a cost (C_c) estimate based on the shaft power of the compressor that is valid between 1.5 and 200 MW. The 1.42 MW main compressor was up-sized to 1.5 MW for cost estimation purposes to fit within the valid domain of the correlation.

$$C_c = 1.23 \times 10^6 \dot{W}_{sh}^{0.3992} \tag{4}$$

The sum of individual component prices only makes up part of the IEC. The piping, valving, and instrumentation also need to be considered, as well as labor costs for installation. For power cycles, it is common to multiply the total equipment price by a factor of 1.3 to obtain an IEC.

Liquid Metal Battery

LMBs are composed of two liquid metal electrodes of different densities, separated by a molten salt electrolyte. As depicted by Fig. 3, during the discharge cycle, anions are transported across the electrolyte to the cathode, where a compound of the two metals is formed. In the charging cycle, the electric potential across the cell pushes ions back to the anode. The technology takes advantage of liquid state mass transport to allow higher current density. [7]

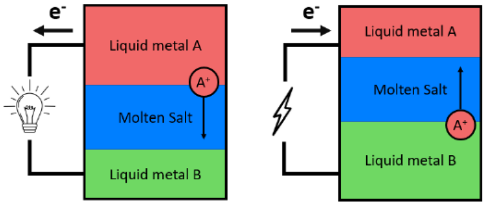

Fig. 3. Schematic drawing of an LMB during (left) discharge cycle and (right) charge cycle [1].

The 20 MWh_e LMB ESS is composed of twenty 1 MWh_e blocks, each composed of 100 cells [1]. The cells are 1 ft by 2 ft with a 1 cm thick antimony cathode and 1 cm thick magnesium anode separated by a 5 cm thick molten chloride electrolyte. The storage block structure is assumed to be 14 gauge 304 stainless steel, with alumina used for electrical insulation. These dimensions and the commodity prices listed in Table A1 of the appendix were used to estimate the cost of raw materials for the LMB. The raw material price was multiplied by a factor of 2 to account for manufacturing costs, and a literature source was consulted to estimate the cost of auxiliary equipment (*e.g.* instrumentation & controls, inverters, rectifiers, and transformers) and installation costs [8].

RESULTS AND DISCUSSION

Fig. 4 breaks the LCOS, LCOE, and LCOH into contributions from CAPEX, fixed O&M, and variable O&M. NRSs are very large capital investments, and the capital expenditure makes up the majority of the LCOH [5]. Power cycles and ESSs are also significant investments, but also have noteworthy contributions from variable O&M.

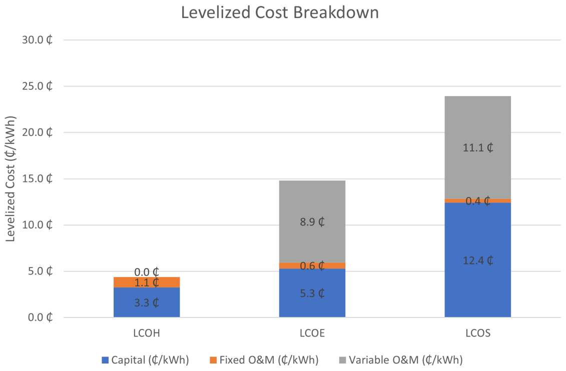

Fig. 4. Breakdown of capital, fixed O&M, and variable O&M to the levelized costs of heat, electricity, and storage.

Levelized Cost of Electricity

The LCOE for the NRS with sCO_2 power cycle was calculated to be 14.9 ¢/kW_e, using a generation price of 8.9 ¢/kW_e, a 20 year project lifetime, 91% capacity factor, and 12% discounting rate. This is on par with the LCOE reported for nuclear power, which is on the high end of the of the spectrum; it is closer to the LCOE from natural gas peaking plants than fossil fuel baseload plants or renewable energy sources. This is promising as it implies that the project is likely to be feasible, but has room to improve with the addition of an LMB.

Levelized Cost of Storage

The LCOS for the LMB was calculated to be 23.5 ¢/kW_e, using a threshold price equal to the generating price of 8.9 ¢/kW_e ('at cost'), a 20 year project lifetime, 1 cycle per day, 12% discounting rate, and a full replacement of the battery cells in year 10. This is close to the LCOS reported for lithium ion batteries [8], indicating that LMBs may be viable if certain advantages that they possess over solid state batteries are highlighted.

Sensitivity Analysis

A sensitivity analysis was conducted to determine how the LCOE and LCOS are affected by key inputs. Figs. 5 and 6 clearly indicate that the LCOE and LCOS are most significantly impacted by changes to the price at the energy purchase price, the size of the initial capital investment, and the utilization of the system.

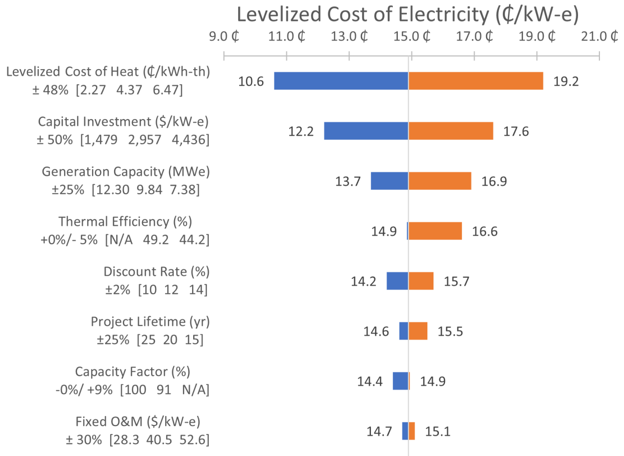

Fig. 5. Tornado chart displaying the sensitivity of the LCOE to changes in various key inputs.

The LCOE from the power cycle is most sensitive to the LCOH from the NRS, which was varied from that of the most cost effective small modular reactor from the literature source [5] to a higher price of equal step size. The baseline assumption for the thermal efficiency was considered to be near the upper bound achievable for this type of power cycle, so it was only penalized by 5%, but not increased. Similarly, the baseline capacity factor of 8000 hr/yr was considered to be low, and it was only increased to 100% for this analysis.

Increasing the TP makes it more likely that the sCO_2 cycle meets the LCOE, but drives up the LCOS. The TP was studied at no cost, at cost, and the LCOE. An increase from 1 to 2 cycles per day was investigated to leverage the strengths of LMBs, and the RTE was varied to assume 100% Coulombic efficiency of the LMB (only considering losses to transformers, rectifiers, and inverters), and to a lower value of equal step size.

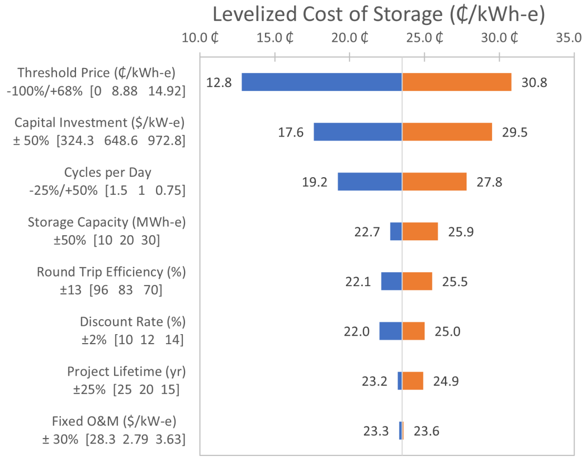

Fig. 6. Tornado chart displaying the sensitivity of the LCOS to changes in various key inputs

FINAL REMARKS

Conclusions

There is a need for NRSs to become more dynamic as decarbonization and renewable energy sources continue to reshape the energy grid. One option to meet these changing demands is to pair the reactor with an ESS. A system composed of a high temperature gas cooled microreactor, sCO_2 power cycle, and LMB compliment each other to provide load following and black-start capabilities to the grid. Current cost estimates for installing the systems yield a competitive levelized cost of electricity and levelized cost of storage, indicating that such a combined system may be economically viable as technological advances lead to them being technically feasible.

Future Work

One of the next steps of this analysis is to further investigate a system such as the one described in this paper using INL's Holistic Energy Resource Optimization Network (HERON) software framework. HERON leverages RAVEN, which generates 'synthetic histories' of certain data sets (notably the price of electricity) to run workflows constructed to meet target economic goals. The frameworks can be used to determine if an ESS is viable in a given market, and can be used to optimize the size of the system using model optimization and regression analysis.

This paper does not consider a potential secondary revenue stream of the LMB: grid spinning reserve capacity payments [9]. Depending on the market, an ESS can receive payments not only for selling electricity to the grid when demand is high, but also by having stored energy available. The value of the grid spinning payment is determined by the amount of energy available and how quickly it can be discharged to the grid. LMBs are able to operate at very high current density, so the cost of larger power equipment will be analyzed to determine if grid spinning payments favor a system capable of more rapid discharge.

ACKNOWLEDGMENTS

This paper and the work described were supported through the INL Laboratory Directed Research and Development (LDRD) Program under DOE Idaho Operations Office Contract DE-AC07-05ID14517.

REFERENCES

1. A. SHIGREKAR, et al., "Modeling and Analysis of NRS Coupled with a LMB," *INL* (2022).
2. E. A. HARVEGO et al., "Evaluation and Optimization of a sCO_2 Power Conversion Cycle for Nuclear Applications," *Conference on Nuclear Engineering* (2011).
3. N. WEILAND, et al., "sCO2 Power Cycle Component Cost Correlations from DOE Data Spanning Multiple Scales and Applications." *ASME* (6 2019), Turbomachinery Technical Conference and Exposition.
4. "Aspen EDR," `www.aspentech.com/en/products`.
5. M. VANATTA, et al., "TEA of SMRs decarbonizing industrial process heat," *Joule*, **7**, *4*, 713–737 (2023).
6. B. A. PINT, "High-Temperature Compatibility of Structural Alloys with Supercritical and Subcritical CO2," *Interface Magazine*, **30**, *2* (6 2021).
7. D. BRADWELL, et al., "Magnesium-Antimony LMB for Stationary Energy Storage," *JACS*, **134**, *4* (2 2012).
8. V. VISWANATHAN, et al., "Grid Energy Storage Technology Cost and Performance Assessment," *PNNL* (2022).
9. M. HUMMON, "DR Resources for Energy and Ancillary Services," *NREL* (2022), CMU Energy Seminar.

APPENDIX

$$NPV = \sum_{t=0}^{n} \frac{FV_t}{(1+i)^t} \tag{A.1}$$

Table A1 contains raw material spot prices obtained for the LMB cost estimate. Eq. (A.1) is the NPV formula given a future value (FV), discounting rate (i), future year (t), and project lifetime (n).

TABLE A1. Commodity Spot Prices

	($/ton)	Link
Mg	8,598	pubs.er.usgs.gov/publication/mcs2022
Sb	11,464	pubs.er.usgs.gov/publication/mcs2022
KCl	520	chemanalyst.com/Pricing-data/1161
NaCl	56	pubs.er.usgs.gov/publication/mcs2022
$MgCl_2$	580	chemanalyst.com/Pricing-data/1403
Al_2O_3	496	pubs.er.usgs.gov/publication/mcs2022
SS304	4,806	agmetalminer.com/metal-prices/